An artificial blood vessel fabricated by 3D printing for pharmaceutical application

Saeid Esmaeili [1], Maryam Shahali [2], Alireza Kordjamshidi [3], Zahra Torkpoor [4], Farshad Namdari [5], Saeed Saber-Samandari [1], Mazyar Ghadiri Nejad [6], Amirsalar Khandan [1]*

[1]*New Technologies Research Center, Amirkabir University of Technology, Tehran, 15875-4413, Iran*
[2]*Department of Quality Control, Research and Production Complex, Pasteur Institute of Iran, Tehran, Iran*
[3]*Department of Pharmacy, Eastern Mediterranean University, Gazimagusa, TRNC, via Mersin 10, Turkey*
[4]*Students Research Committee, School of Medicine, Isfahan University of Medical Sciences, Isfahan, Iran*
[5]*Department of Urology, AJA University of Medical Sciences, Tehran, Iran*
[6]*Department of Industrial Engineering, Eastern Mediterranean University, Gazimagusa, TRNC, Via Mersin 10, Turkey*

ABSTRACT

Objective(s): Cardiovascular diseases (CVDs) are the leading cause of mortality in the elderly. A common medical procedure for the treatment of CVDs is the replacement of the blocked or narrowed arteries, which is currently the optimal vascular transplant associated with autograft transplantation. In general, the saphenous veins and radial arteries in the mammary gland are considered to be the selective vessels for vascular substitution. In many cardiac patients, artificial blood vessels (ABVs) are not used for several reasons, including the age of the patient, small size of the veins, previous impressions, and abnormally. Therefore, the consideration of vascular substitute demands is inevitable, especially regarding vascular transplantation with very small diameters and availability of proper alternatives. The present study aimed to develop a novel artificial bio-composite blood vessel using polymer-reinforced and bioceramic nanoparticles.

Materials and Methods: The biomechanics and chemical properties of artificial vessels have been investigated to be used in coronary artery bypassing in atherosclerosis as a soft tissue engineering procedure. In this study, thermoplastic polyurethane (TPU) composed of nanocrystalline hydroxyapatite (HA) nanopowder was prepared using the extrusion technique to construct the ABVs. X-ray diffraction (XRD) and scanning electron microscopy (SEM) were used to investigate the optimum specimen. An important feature of the ABVs was the ability to find the elastic modulus, wettability, and porosity of the veins, which were assessed by fused deposition modeling and 3D printing.

Results: The sample containing five wt% of HA had superior mechanical and biological features over the pure sample.

Conclusion: According to the results, the narrowed arteries composed of TPU composite with nanocrystalline HA nanopowder had proper chemical stability and mechanical characteristics.

Keywords: *Artificial vessel, 3D Printing, Flexible polymer, Bioceramic, Cardiovascular Diseases*

INTRODUCTION

Within the past decades, cardiovascular diseases (CVDs) have been the leading cause of human mortality and morbidity throughout the world. A common medical procedure for CVDs is the replacement of the blocked or narrowed portion of the arteries. In several cases, the veins in the patient's body should be substituted for some reasons, such as the age of the patient, small size of the veins, varicose, and other disorders [1-3]. The demand for alternative vessels (e.g., small diameters of the vascular graft) is inevitable [4-5]. On the other hand, the importance of innovation and knowledge management orientation is undeniable in every health system. Today, tissue engineering aims to design and fabricate artificial veins with maximum

adaptation to the natural arteries. In 1912, Carrel first studied the use of metal and glass tubes as an artificial artery in cardiac surgery of dogs [1-7]. Another research conducted by Jiang *et al.* [3] aimed to fabricate and characterize a polymer nanoparticle substrate, which could be used in artificial arterial replacement by electrochemical polycaprolactone (PCL). The mentioned study evaluated the accuracy of artificial arterial replacement with surface oxygen plasma and acrylamide transplantation. In order to provide a proper bedding for the production of the artificial replacements for the vessels that had lost their ability, the researchers produced a modified PCL nanostructure and activated the surface by oxygen plasma [4]. According to the literature, the PCL fibers and monosaccharides that are used in CVD treatment may lead to cardiac arrest and death in severe cases. The formation and precipitation of fatty masses layer in the walls of the veins is considered to be the most important parameter in the development of arterial cramps.

Currently, use of drugs is the first option for the treatment of patients with CVD. However, when the clogging of the veins is extremely severe and cannot be remedied by medical and angiographic methods, the pathway should be replaced with bypass and vessel transplant surgeries [4-6]. In addition, cardiac arrest cannot be easily prevented. Cardiac arrest is a complicated condition for surgeons and patients, and the patients may suffer from prolonged postoperative pain [7, 8].

The first step in the preparation of artificial veins is to select the proper biological material in order to incorporate the most proper features of the human vein. Selection of these biological materials is based on the biocompatibility and identity of the materials that are of a natural sources with logical mechanical and chemical stability [9-12]. In a study in this regard, Mostafavi *et al.* [4] examined the issue of using polymer materials (e.g., Teflon, polyesters, and polyurethanes prostheses) due to their lack of anticoagulant properties and the restricted use in the veins with higher diameters than six millimeters. The risk of blood clotting and ability to build artificial arteries with high strength and durability remain a matter of debate between polymer engineers and chemists. Researchers attempted to design an artificial vein using a Teflon membrane as a natural polymer and optimized the porosity and fluid transmissions [10-11].

The present study aimed to fabricate and

characterize a novel artificial bio-nanocomposite array produced by fused deposition modeling (FDM) or fused filament fabrication (FFF) as an additive manufacturing technology for medical approaches, which was composed of thermoplastic polyurethane (TPU, matrix) and nanocrystalline hydroxyapatite (HA) additive filler with varibale amounts in order to construct multibranch ABVs for application in the treatment of CVDs for the first time.

MATERIALS AND METHODS
Material preparation

In order to fabricate an artificial vein in this research, the making of the filament was performed in three separte phases. In the first phase, the artificial vein specimen was designed and manufactured using an FDM printer. In addition, the nanocrystalline HA powder was produced using a bovine bone, which was milled for 10 hours. The nanopowder was subjected to heat treatment at the temperature of 800-850°C for three hours in order to remove the impurities.

Fig 1 depicts a schematic view of the technique applied to produce the raw materials and TPU with 0, 2.5, 5, and 7.5 wt% of the reinforcement that was mixed with nHA and ground for two hours using a planetary high energy ball mill (HEBM). The TPU polymer was ground using a cutter machine so as to obtain a smaller size. Afterwards, a specific concentration of the HA powder (CAM Company; 50-100 nm, 98% purity, crystalline) was added to the TPU polymer, and the mixed nanocomposite was soaked in the TPU solution and stirred for four hours using a magnetic stirrer. Following that, the prepared solution was ultrasonically homogenized to avoid the precipitation of the HA powder. The homogenized solution was inserted into an extrusion machine, where the filament (1.75 mm) was produced. The prepared filament was rolled on the hot coil in order to prevent solidification or degradation. Finally, the filament was inserted into the FDM machine to develop the artificial veins with the diameter of six millimeters.

Some of the prominent properties of TPU polymer include high strength, biocompatibility, non-adhesion, and high polarity due to the presence of the fluorine atom in its structure. On the other hand, this polymer has wear resistance and lack of clarity in various solvents. Owing to its favorable mechanical properties, lack of biological changes in the body, and no reaction to blood

184

Nanomed. J. 6(3):183-194, Summer 2019

components, TPU is considered to be an optimal polymer in the manufacturing of vascular grafts.

Fabrication of the filament

In order to fabricate the filament, TPU with HA ceramic material was purchased from Merck Company. After mixing TPU and HA for four hours, the obtained combination was inserted into the extruder and heated at the temperature of 210-220°C from the extruder nozzle to produce a filament with the diameter of 1.75 millimeters. When the material exited, the desired filament for the development of an artificial vessel was prepared using a 3D printer.

Design and fabrication of the artificial artery

In the designing process of the vessel specimen, an inner diameter of four millimeters was developed as the vein duct to a moderate extent proportional to the large body of the veins in the body. In addition, an outer diameter of six millimeters and a wall with the vein thickness of 100-150 microns were designed. The total length of the designed cylinder was 12 millimeters using the FDM machine. For the feasibility of the fabrication, several branches of the ducts (e.g., ductwork design) were also designed with interference between the two ducts. The Solid Works software was used for the designs, and the STL file was stored for the fabrication phase by a 3D printer.

To prepare the 3D printed FDM, the table temperature was initially set at 70°C, and the extruder nozzle temperature was set at 210-220°C. For non-intrusive and leaking fluids, the device was adjusted to 100 microns, and the quality of the process was selected in the *"Simplify3D"* software. Following that, the device was ready for G-coding. After the encoding, the program was started for the 3D printing of the artificial arteries composed of TPU and HA. The nozzle diameter was 20% millimeter with the extrusion width of 0.36 millimeters.

Material characterization

X-ray diffraction (XRD) was used to evaluate the phase structure of the starting materials. This process was performed at Amirkabir University of Technology in Tehran, Iran within the range of 10-90º. Moreover, scanning electron microscopy (SEM) was utilized to evaluate the morphology of the pure materials before and after the

composition. The structural morphology and surface images of the bio-nanocomposite scaffolds were captured using the SEM equipment.

The samples were coated with gold (Au) by sputter spraying (SC7620 type, Quorum technologies-EMITECH) for 200 seconds with low vacuum at 80-120 V accelerating voltage of 30 mA (SERON technologies, AIS2100, South Korea) at Amirkabir University of Technology. The XRD pattern indicated that n-HA was a nanocrystalline material, and the sharp peaks were designated at 2θ of ≈27˚, 32˚, 42˚, 44˚, and 47˚ to match the original XRD of HA with the standard card number of JCPDS 0432-009 for nanocrystalline HA within the range of 70-90 nanometers based on the modified Scherrer equation [47]. In addition, the morphology and structure of the HA-TPU bio-nanocomposite were characterized via XRD and SEM.

Mechanical properties

Designed vein vessels that are to be used in the body require relatively high resistance to tear and proper elongation at the bending point. To examine the artificial arteries made by the 3D printer and determining their mechanical properties, a vessel sample was developed using the jaws of the SANTAM-STM 50 model based on the ASTM standard, and the required diagrams were plotted. The elastic modulus was extracted from the region with maximum stress-strain slope before failure, and the extracted elastic modulus was 10-30. Afterwards, a micromechanical model was applied to the experimental values, including the Dewey model (DM), Rice model (RM), Herakovich and Baxter model (HBM), Gibson model (GM), Roberts and Garboczi model (RGM), Ramakrishnan and Arunachalam model (RAM), and differential scheme (DS) model. These models are presented in Equations 1-8 and were used to predict the correlation between the elastic modulus and porosity values.

Biocompatibility properties

In order to assess the biological properties of the TPU veins reinforced with the HA particles, a piece of the vessel (length: 20 mm) was separated from the samples and stored for in 5% acetic acid solution and 10% saline water solution for 21 days, and the obtained results were investigated. To evaluate the biocompatibility of the produced vessel, the specimens were tested

Nanomed. J. 6(3):183-194, Summer 2019

185

for 21 days at the temperature of 37°C (human body temperature) using simulated body fluid (SBF), which was prepared through the Kokubo procedure (Table 1) [23].

Table 1. Comparison of base elements in SBF solution with human blood plasma

Ion	SBF (mM)	PS (mM)	Human plasma (mM)
Na^+	142.0	153	142.0
K^+	5.0	-	5.0
Mg^{2+}	1.5	-	1.5
Ca^{2+}	2.5	-	2.5
Cl^-	147.8	153	103.0
HCO_3^{3-}	4.2	-	27.0
HPO_4^{2-}	1.0	-	1.0
SO_4^{2-}	0.5	-	0.5
pH	7. 4	5.2	7. 2 -7. 4

RESULTS AND DISCUSSION

In the microstructure evaluation of the ABVs, similar to the current prosthetics, an intelligent physical hypothesis was applied *in-vitro*, and the model analysis is depicted in Fig 1.

The TPU biopolymer was mixed with various concentrations the HA power (0, 2.5, 5, and 7.5 wt%) in a high-energy ball milling machine. Following that, the mixed composite powders were inserted into the extrusion machine at a specific heating rate.

Afterwards, the obtained results with the homogenized TPU-HA filament were extracted and inserted into the 3D printing machine.

To evaluate the ABV structure, the mechanical and biological properties were evaluated, and the results were compared to the analytical models.

According to the results, the biodegradability of the polymeric tissue changed, thereby affecting the mechanical properties of the materials.

Gao *et al.* [9] introduced stress analysis in a layered aortic arch model under pulsatile blood flow, proposing the blood vessel length of 0.025 meter with the density of 1090 kg/cm³ and Poisson's ratio of 0.45. In the mentioned research, the ABV could function in the human body several times, tolerating the pressure induced by high blood pressure and the pulmonary movement of the vein.

The results of the bioassays indicated that the coagulation time of the biochemical materials improved 10-fold, which corresponded to that of the prosthetics on the market.

Furthermore, other functional tests (e.g., mechanical tests, cytotoxicity, and biocompatibility) confirmed that these materials could be applied in the production of ABVs for the human body. Despite the efforts to find alternative materials for cardiovascular diseases, failure due to the use of materials such as metals, glass, and silk is considered to be the main reason for the use of synthetic materials.

Recently, complications such as blood clotting and interaction minimization of blood and tissue have attracted the attention of researchers. To date, more than 100 natural and artificial polymers have been electrolyzed for ABV applications; however, only a few have been approved by the American Food and Drug Administration (FDA) for use in human clinics [13-18].
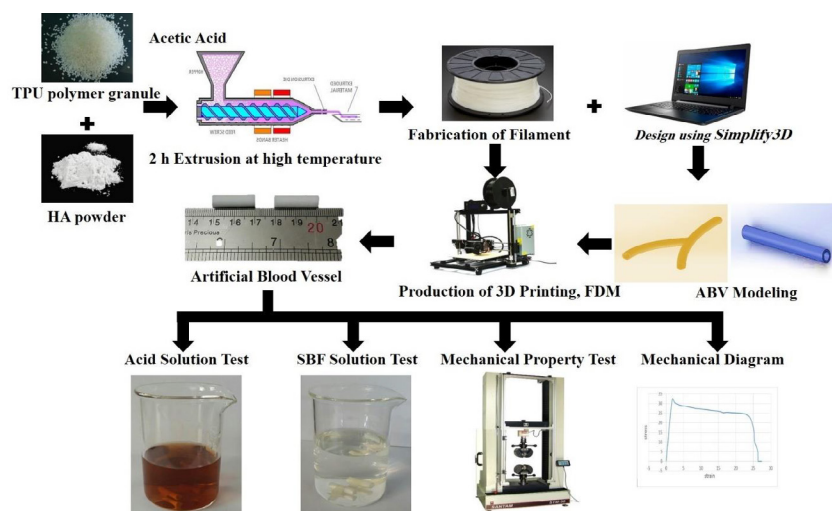

Fig 1. Schematic design and construction of dual-component bio-nanocomposite ABV using 3D printer machine, HA powder, and TPU polymer

Some of the approved polymers for vascular substitution by the FDA include polyethylene terephthalate (Dacron), polytetrafluoroethylene (Teflon) [10], and polyurethane, which are commonly utilized in tissue engineering using various technique like 3D printing and freeze drying [17-26, 34].

The patients with peripheral arterial and kidney diseases who suffer from arterial cramps and loss of vein function are classified as candidates for angioplasty (balloon angioplasty), endarterectomy, and bypass grafting. In some cases, the patient lacks the proper vein structure for self-sustaining (providing a transplant from the patient's body) and operation. Polyurethanes are the proper materials for ABV construction in these patients owing to their blood compatibility [18-22]. The biocompatibility and ability of these materials to mimic the human body play a key role in this regard. In the present study, we investigated the fabrication of TPU-based synthetic ABV based on the modification of the main chain chemical microstructure using the HA bioceramic [27-35]. Additionally, the effects of the materials and techniques used to manufacture an ABV with proper mechanical and chemical properties (e.g., toxicity, endothelial adhesion, and platelet adhesion) were evaluated. According to the findings, the application of biodegradable polymers (e.g., TPU and PCL) with prolonged degradation increased porosity at the level of the substitute scaffolds composed of the HA powder compared to the pure materials [36-39].

In case of vessels with small diameters, Dacron scaffolds still account for a high failure rate due to surface traction forces and the absorption of proteins from the plasma by the scaffolds [40-44].

Conventional ABVs are susceptible to inflammation, infections, thrombosis, and blockage after implantation. In general, the scaffolds produced from Dacron compilation have exhibited slight resilience, which leads to failure in the fabrication process of ABVs with small diameters.

On the other hand, the new biotech ABVs are tight, flexible, and resistant to clotting, while they also have an adaption system to heart palpitations based on nanotechnology and the loading of specific microscopic molecules inside the bonds. Utilization of atomic- and molecular-level analytical materials along with nanotechnology enables these thorns to the magnetic core (stem cells). When stem cells are absorbed, they cover the entire inner surface of the stem and become endothelial cells. Use of these polymeric materials enables transplantation in human ABVs, helping deliver nutrients to the tissues of the body. The ultimate goal is to use these links in the coronary and lower-extremity arteries to reduce the risk of cardiac arrest and amputation.

In 2014, Zhou et al. [11] used silk fibers combined with polyurethane polymer, and the obtained results indicated that the biocompatibility of the substance increased, while all the polyurethane specimens had low-range toxicity, which improved proper biocompatibility. In addition, polyurethanes showed high biocompatibility and non-toxicity compared to polytetrafluoroethylene. Several examples of these biopolymers have been reported by bioengineers, including the delivery of drugs and genes, ABVs, artificial limbs, and facial masks [27-30]. For instance, hollow carbon fibers with smaller diameters than the blood vessels are greatly suitable for intravascular drug administration [31]. These nanofibers could also be used for medical applications, such as the bandages and sutures that are completely dissolved in the body [32-35]. The aim of applying these nanofibers is to minimize the risk of infections and achieve complete absorption in the body. Considering the larger size of red blood cells (approximately 7 μm) compared to nano-matrix cavities, these cells cannot cross nano-matrix cavities. On the other hand, the hollow carbon fibers that are less diagonal than blood vessels are viable options for carrying intravaginal drugs.

Nanofibres and the network they form are capable of the direct delivery of drugs to the internal tissues. Several studies have been focused on various weight fractions of the materials that are used in soft pieces. For instance, Martin et al. [20] employed the combination of the polyester polymers of poly-hexamethylene oxide and bridge polydimethylsiloxane as a smooth piece and determined their optimal biocompatibility and flexibility [20, 36-37].

Table 2. Mechanical and Geometric Properties of Aortic Vessel [10-11,38]

	Blood Vessel Length (m)	(kg/m^3) Density	(m) Outer Radius	(m) Inner Radius	Poisson's Ratio
Value	0.025	1090	0.0123	0.0125	0.45

Table 2 shows the comparison of the mechanical properties of polyhedral oligomeric silsesquioxane poly(carbonate-urea) urethane (POSS-PCU) and some commercial bridges [10, 38].

Among the prominent features of these artificial arteries were strength and flexibility. The obtained results regarding mechanical properties of various ceramic additive contents are shown in Table 3.

Table 3. Physical and mechanical properties of ABV designed by FDM using TPU reinforced with HA powder

Mechanical Properties	0 wt%	2.5 wt%	5 wt%	7.5 wt%
Porosity (%)	36	46	46	41
Elastic Modulus (MPa)	1680	1620	1580	1526
Density (gr/cm^3)	1.12-1.24	0.42	0.52	0.63
Tensile Strength (MPa)	3.1	2.2	3.6	3.7
Poisson's Ratio	0.45	0.34	0.35	0.35

ABVs should be able to provide biocompatibility and non-toxicity resistance in infections. Additionally, ABVs should possess mechanical and blood compatibility similar to polyurethane. Among other properties of TPU-based ABVs is resistance to infections and FDA approval, which is considered to be an important criterion since the implant may cause infections after installation [39-42]. Therefore, most surgeons use large amounts of antibiotics (e.g., gentamicin and triclosan) during and after ABV implantation surgeries, while high levels of antibiotics may lead to various complications, such as bacterial resistance, hypersensitivity, and metabolic disturbances [22].
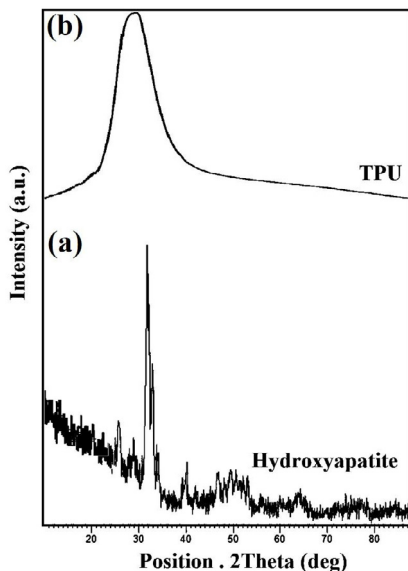

Fig 2. Comparison of XRD pattern of a) HA powder and b) TPU polymer in current research

Figs 2a and 2-b show the XRD pattern of the bioceramic and biopolymer used in the present study.

High accumulation of ceramic nanoparticles in living organisms causes various disabilities and diseases in the blood, as described by the previous model [43, 44].

The application of magnetite nanoparticles in bioceramic has been investigated, and the biological properties have been confirmed. Therefore, it is possible to use magnetite and copper nanoparticles in the structure of ABVs [45, 48].

Furthermore, the wettability of the vessel is another important factor in the evaluation of ABV in terms of blood diffusion and penetration [46].

In the current research, cell viability and cell attachment were investigated with the addition of copper oxide nanoparticles to the HA bioceramic. According to the findings, the copper oxide nanoparticles could enhance cell attachment and cell growth [47].

It is notable that other trace elements (e.g., carbon nanotube [CNT]) may increase the strength of the structure [48-52].

Figs 4-a-d demonstrate the designed ABV in the present study using TPU and HA powder with one and two branches.

As is depicted in Fig 4-b, a triangular motion of the FDM machine could prepare a more homogenized and continues vessel compared to the other motions with higher porosity.

This method could be used to monitor and control the porosity of the ABV wall as well. The top and lateral views of the two-branch ABV indicated the thickness of the product to be 100-150 microns, while the outer diameter of the vein was six millimeters.

Figs 5a-b show the mechanical values measured using SANTAM-STM 50 in the samples with various concentrations of the HA powder. Accordingly, the Young's modulus of the sample increased from 15 to 21 MPa with the addition of the HA powder to TPU.

The increased elastic modulus of the composite could be due to the higher Young's modulus of HA compared to TPU.

Moreover, the hardness value was observed to increase from 0.3 to 0.63 (N) with increasing the concentration of the HA powder in the TPU polymer.
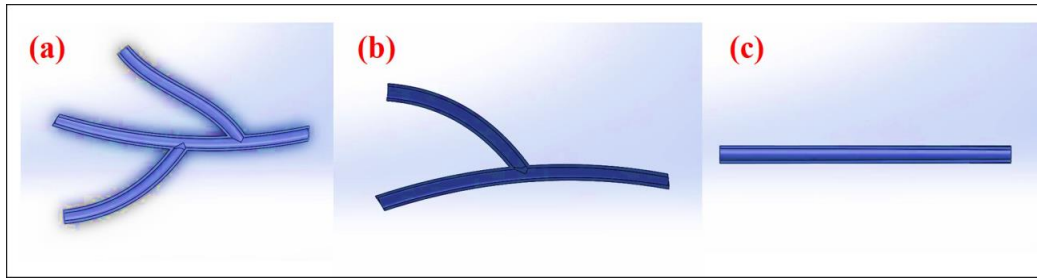
188

Nanomed. J. 6(3):183-194, Summer 2019

Fig 3. ABV designed in CAD software; a) Multiple branches, b) Two branches, and c) Single branch using solid work software
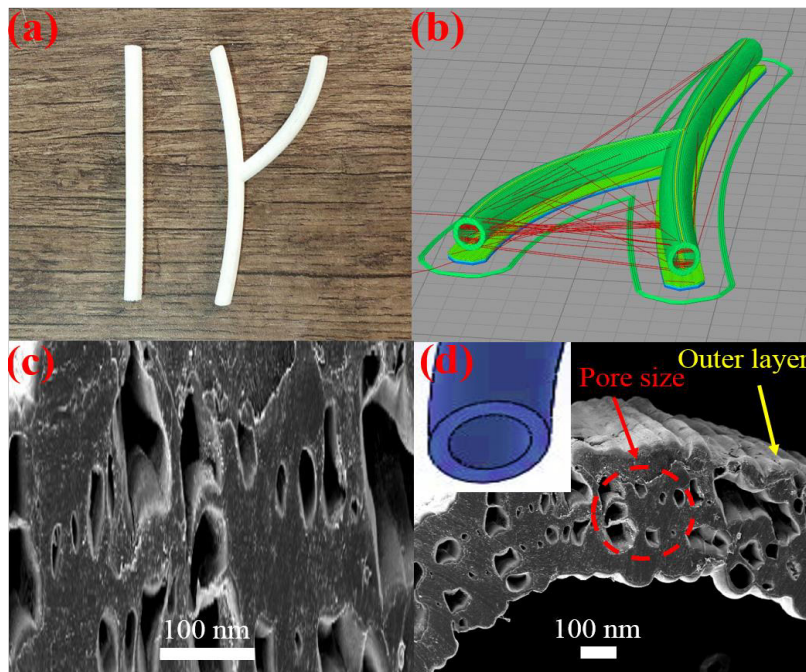

Fig 4. a) Designed two-branch ABV, b) Approaches to designing vessels in solid works software and ABV model in Simplify 3D software, c) Top of SEM image and d) Lateral view of SEM image constructed by 3D printer (pore size: 50-100 microns)
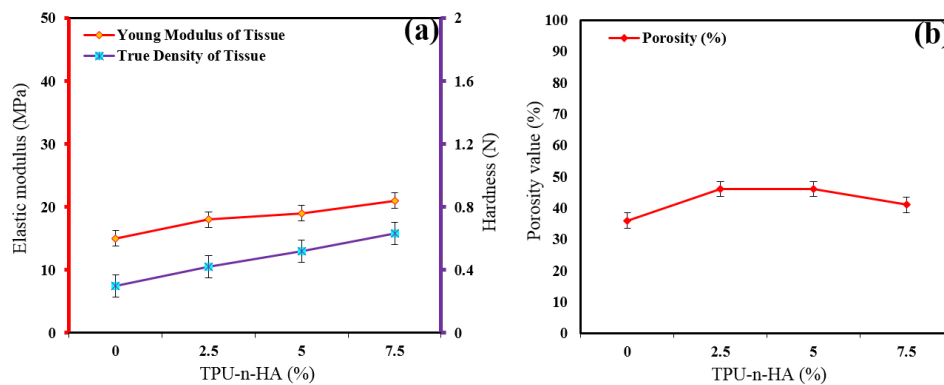

Fig 5. Diagram of a) Elastic modulus versus hardness and b) Porosity of bio-nanocomposite tube

Although the porosity results indicated an increment in porosity from 36% to 41%, the porosity remained constant in the samples containing 2.5 and 5 wt% of HA (Fig 5-b).

Figs 6a-b illustrate the Ca ion concentration of the specimen soaked in SBF for 21 days at the temperature of 37°C in an incubator. According to the obtained results, the Ca^{2+} ion decreased after 21 days.

As is depicted in Fig 6-a, the pH of the sample

Nanomed. J. 6(3):183-194, Summer 2019

189

remained constant after 21 days of incubation in SBF saline. Only after the first and second week, some fluctuations were observed in the samples with 2.5 and 5 wt% of HA in terms of the Ca ion concentration and PO_4 group of HA.

Figs 7a-c represent the soaking environment of the samples in acid solution (pH=4) and base solution (pH=12) for 21 days.

The obtained results are shown in Fig 6a, in which the sample with higher HA powder is observed to have higher chemical stability compared to the sample without the HA powder.

According to the results of the present study, the concentration of HA increased in the TPU structure, while the biodegradation and dissolution of HA in the composite remained constant in terms
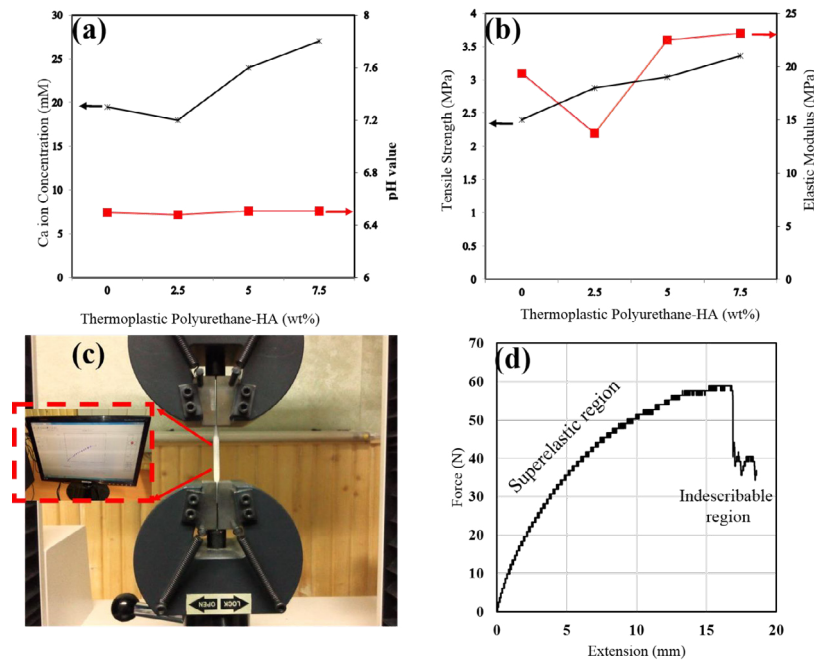

Fig 6. Diagram of a) Ca2+ ion concentration versus pH changes, b) Tensile strength versus elastic modulus, c) Tensile machine, and d) Stress-strain curve of bio-nanocomposite ABV tube

Fig 7. Results of biological testing of artificial bio-nanocomposite made by 3D printing soaked in a) Acid solution, b) Sample fixation in saline solution, and c) SBF solution for 21 days

Table 4. Comparison of mechanical properties of existing commercial multi-bridge ABVs and POSS-PCU [10-11, 21]

Material	Tensile strength (N/mm^2)	Tear strength (N/mm)	Hardness (Shore A)	Elongation at tear (%)
Estane (PEU)	48.3	55	85	570
Chronoflex^c	45.5-37.9	45	80	400-490
Elast-Eon^{TM}	20-30	50-80	75-90	500-570
POSS-PCU	53.6±3.4	50±1.2	84	704.8±38

190

Nanomed. J. 6(3):183-194, Summer 2019

of the adhesion between the polymer and ceramic at the outset of the production system.

Comparison of the mechanical properties of the existing commercial multi-bridge ABVs with laboratory ABVs is presented in Table 4.

According to the information in Table 4, the Elast-Eon and collagen in the wall of the scaffolds increased compilation, strength, and flexibility, thereby resulting in absorbable vascular scaffolds and sutures in the natural blood vessels. Therefore, TPU was observed to be biocompatible and non-toxic substance, which could improve the chemical properties of the synthetic scaffolds, as well as their mechanical properties, which are essential to the preparation of optimal vertebrate blood grafts. In addition, these bio-scaffolds are less thrombogenic compared to Teflon scaffolds and have superior biocompatibility with the host soft tissue. Another prominent feature of these scaffolds is adequate resistance to the dialysis process [10].

According to the micromechanical model that correlated the porosity of the bio-nanocomposite with the elastic modulus of the ABV materials in the current research, the DM was applied successfully to the TPU-HA samples using equations 1-a and 1-b, as follows [51-53]:

$$\frac{E_p}{E_s} = 1 - \xi\phi \quad (a) \qquad \xi = \frac{(1-v_s)(27+15v_s)}{(2(7-5v_s))} \quad (b) \qquad \text{Eq. 1-a, 1-b}$$

In addition, the RM could be applicable in the RM model, in which the R-value was estimated at 0.5 based on laboratory tests and Equation 2.

$$\frac{E_p}{E_s} = 1 - \exp(-r(1-\phi)) \qquad \text{Eq. 2}$$

Another technique based on the HBM was applied based on the generalized method of cells model for the spherical shapes and porous structures to evaluate the Ep/Es ratio as shown in the SEM images. The SEM images revealed the HA and TPU that were mixed uniformly in the 3D printing machine, with ϕ representing the porosity ratio of the samples, which was approximately 30-40% based on Equation 3, as follows:

$$\frac{E_p}{E_s} = 1 - 1.15\phi^{2/3} \qquad \text{Eq. 3}$$

Equation 4 shows the GM formula, which was employed to evaluate the aspect ratio of semi-porous materials to the solid form, with the η

value estimated at two and three for the open and close porous structures, respectively [50-51, 53].

$$\frac{E_p}{E_s} = \frac{\rho_p}{\rho_s} = (1-\phi)^\eta \qquad \text{Eq. 4}$$

In the current research, RGM was used with the initial values such as the elastic modulus of the porous and dense forms, where m (0.818, 0.798), n (2.25, 1.65), a (0.166, 0.221), and b (0.84, 0.604) were extracted from the experimental tests introduced in the RGM theory for elliptical and spherical shapes (Equations 5a-b).

$$\frac{E_p}{E_s} = (1 - \frac{\phi}{m})^n \quad (a) \qquad v_p = a + (1 - \frac{\phi}{b})(v_s - a) \quad (b) \qquad \text{Eq. 5a-b}$$

RAM is able to predict the elastic modulus of porous materials with the porosity of less than 40% and higher accuracy compared to other models.

$$\frac{E_p}{E_s} = \frac{(1-\phi)^2}{(1+\chi\phi)} \quad (a) \qquad \chi = 2 - 3v_s \quad (b) \qquad \text{Eq. 6a-b}$$

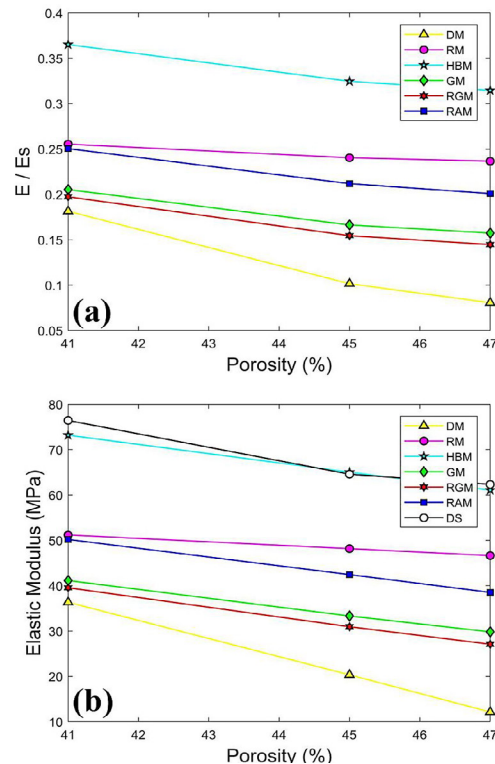The DS model was the last model appropriate for the TPU-HA bio-nanocomposite vein as shown in Fig 8(a-b).

Fig 8. Prediction of a) E/Es and b) Elastic modulus of composite sample at various porosity rates containing HA particle in TPU using 10 classic available models

Nanomed. J. 6(3):183-194, Summer 2019

191

$$\frac{(1+\frac{4\mu_s}{3\kappa_s})(\frac{\mu_p}{\mu_s})^3}{2-(1-\frac{4\mu_s}{3\kappa_s})(\frac{\mu_p}{\mu_s})^{\frac{3}{5}}}=(1-\phi)^6 \quad (a) \qquad \frac{\mu_p}{\mu_s}=\frac{(1-\frac{4\mu_p}{3\kappa_p})^{\frac{5}{3}}}{(1-\frac{4\mu_s}{3\kappa_s})^{\frac{5}{3}}} \quad (b) \qquad Eq.\ 7a\text{-}b$$

$$\frac{(1+\frac{4\mu_s}{3\kappa_s})(\frac{\mu_p}{\mu_s})^3}{2+(\frac{4\mu_s}{3\kappa_s}-1)(\frac{\mu_p}{\mu_s})^{\frac{3}{5}}}=(1-\phi)^6 \quad (c) \qquad \frac{\mu_p}{\mu_s}=\frac{(\frac{4\mu_p}{3\kappa_p}-1)^{\frac{5}{3}}}{(\frac{4\mu_s}{3\kappa_s}-1)^{\frac{5}{3}}} \quad (d) \qquad Eq.\ 7c\text{-}d$$

In the cases where Equations 7a-b were used for higher Poisson's ratios than 0.2 and lower Poisson's ratios than 0.2, Equations 7c-d were also applicable. The elastic modulus and Poisson's ratio of the porous materials in the DS model were calculated using Equations 8a-b, as follows:

$$E_p=\frac{9\kappa_p\mu_p}{3\kappa_p+\mu_p} \quad (a) \qquad v_p=\frac{3\kappa_p-2\mu_p}{2(3\kappa_p+\mu_p)} \quad (b) \qquad Eq.\ 8a\text{-}b$$

The solution used with the micromechanical modeling to dissolve the cardiovascular vein with the TPU polymer and bioceramic was simulated.

CONCLUSION

CVDs are considered to be a major cause of mortality worldwide. The replacement of blocked or narrowed arteries is a common medical procedure for the treatment of CVDs and is currently the optimal vascular graft for autograft transplantation. In general, artificial veins are considered as selective vessels for vascular replacement, while in many cardiovascular patients, the veins have numerous problems for several reasons, including the age of the patients, small size of the veins, previous impressions, and abnormalities. Therefore, the demand for alternative artificial vessels, especially vessels with very small diameters, must be addressed inevitably.

Today, tissue engineers plan to design and construct artificial vessels with maximum compliance with natural veins. Artificial insemination should provide biocompatibility, non-toxicity, and resistance to infections, while maintaining their mechanical properties and blood coagulation. TPU and HA are biomaterials that are highly capable of providing these benefits; however, they need to be improved in terms of some biological and mechanical properties. Despite the efforts to synthesize TPU with acceptable properties and enhance its properties with chemical modifications at the surface or mass levels, further success could be achieved in this regard. With proper corrections to improve the properties of ABVs on TPU, these materials could be used in the manufacturing of actual blood vessel.

Changes in shear stress in microorganisms alter the penetration and mass deposition within the microorganisms due to damage to the endothelial layer; this may be an influential factor in the formation of fat cells, thereby giving rise to cardiac diseases. Given the importance of the subject, the present study aimed to examine the influential factors in the shear stress on the microwave wall, elastic modulus, and porosity of ABVs. According to the findings, the combination of the analytical model and experimental evaluation could be utilized to simulate the micromechanical behavior of arterial blood vessels. It is also notable that the porosity of blood vessels significantly affects the shear stress and elastic modulus of the veins. In this regard, out findings indicated the significant effect of the rheological behavior of blood on shear stress variations.

The results of the present study demonstrated the effect of the obstruction rate, location of the pores, and degree of reinforcement in the veins on the elastic modulus and porosity of the tube. Moreover, the biological behavior of the specimens indicated that the addition of bioceramic could enhance the elastic modulus response of the tubes.

ACKNOWLEDGEMENTS

REFERENCES

1. Yancopoulos GD, Davis S, Gale NW, Rudge JS, Wiegand SJ, Holash J. Vascular-specific growth factors and blood vessel formation. Nature. 2000; 407(6801): 242.
2. Ahmed M, Hamilton G, Seifalian AM. The performance of a small-calibre graft for vascular reconstructions in a senescent sheep model. Biomat. 2014; 35(33): 9033-90340.
3. Jiang YC, Jiang L, Huang A, Wang XF, Li Q, Turng LS. Electrospun polycaprolactone/gelatin composites with enhanced cell–matrix interactions as blood vessel endothelial layer scaffolds. Mater Sci Eng C Mater Biol Appl. 2017; 71: 901-908.
4. Mostafavi F, Golshan Ebrahimi N. Physical characterization and rheological behavior of polyurethane/poly (caprolactone) blends, prepared by solution blending using dimethylacetamide. J Appl Polym Sci. 2012; 125(5): 4091-4099.
5. Kapadia MR, Popowich DA, Kibbe MR. Modified prosthetic vascular conduits. Circulation. 2008; 117(14): 1873-1882.
6. Lutolf MP, Hubbell JA. Synthetic biomaterials as instructive extracellular microenvironments for morphogenesis in tissue engineering. Nature Biotechnol. 2005; 23(1): 47.

192

Nanomed. J. 6(3):183-194, Summer 2019

7.Vaz C, M Van, Tuijl S, Bouten C V C, Baaijens F P T. (2005). Design of scaffolds for blood vessel tissue engineering using a multi-layering electrospinning technique. Acta Biomater. 1(5), 575-582.

8.Griffith LG, Naughton G. Tissue engineering current challenges and expanding opportunities. Science. 2002; 295(5557): 1009-10014.

9.Gao F, Watanabe M, Matsuzawa T. Stress analysis in a layered aortic arch model under pulsatile blood flow. Biomed Eng Online. 2006; 5(1):25.

10.Harrison JH. Synthetic materials as vascular prostheses: II. A comparative study of nylon, dacron, orlon, ivalon sponge and teflon in large blood vessels with tensile strength studies. Am J Surg. 1958; 95(1): 16-24.

11.Zhou M, Wang WC, Liao YG, Liu WQ, Yu M, Ouyang CX. In vitro biocompatibility evaluation of silk-fibroin/polyurethane membrane with cultivation of HUVECs. Front Mater Sci. 2014; 8(1): 63-71.

12.Heydary HA, Karamian E, Poorazizi E, Heydaripour J, Khandan A. Electrospun of polymer/bioceramic nanocomposite as a new soft tissue for biomedical applications. J Asian Ceram Soc. 2015 ;3(4): 417-425.

13.Heydary HA, Karamian E, Poorazizi E, Khandan A, Heydaripour J. A novel nano-fiber of Iranian gum tragacanth-polyvinyl alcohol/nanoclay composite for wound healing applications. Proc Mater Sci. 2015; 11: 176-182.

14.Salami MA, Kaveian F, Rafienia M, Saber-Samandari S, Khandan A, Naeimi M. Electrospun polycaprolactone/lignin-based nanocomposite as a novel tissue scaffold for biomedical applications. Med Signals Sens. 2017; 7(4): 22.

15.Khandan A, Jazayeri H, Fahmy MD, Razavi M. Hydrogels: types, structure, properties, and applications. Biomat Tiss Eng. 2017; 4: 143-169.

16.Razavi M, Khandan A. Safety, regulatory issues, long-term biotoxicity, and the processing environment. In Nanobiomat. Sci Dev Eval. 2017(pp. 261-279). Woodhead Publishing.

17.Kordjamshidi A, Saber-Samandari S, Nejad MG, Khandan A. Preparation of novel porous calcium silicate scaffold loaded by celecoxib drug using freeze drying technique: Fabrication, characterization and simulation. Ceram Int. 2019.

18.Saber-Samandari S, Afaghi-Khatibi A. Evaluation of elastic modulus of polymer matrix nanocomposites. Polym Compos. 2007; 28(3): 405-411.

19.Saber-Samandari S, Saber-Samandari S, Kiyazar S, Aghazadeh J, Sadeghi A. In vitro evaluation for apatite-forming ability of cellulose-based nanocomposite scaffolds for bone tissue engineering. Int J Biol Macromol. 2016; 86: 434-442.

20.Martin DJ, Warren LA, Gunatillake PA, McCarthy SJ, Meijs GF, Schindhelm K. Polydimethylsiloxane/polyether-mixed macrodiol-based polyurethane elastomers: biostability. Biomat. 2000; 21(10): 1021-1029.

21.Kidane AG, Burriesci G, Edirisinghe M, Ghanbari H, Bonhoeffer P, Seifalian AM. A novel nanocomposite polymer for development of synthetic heart valve leaflets. Acta Biomater. 2009; 5(7): 2409-2417.

22.Bonesi M, Kennerley AJ, Meglinski I, Matcher S. Application of Doppler optical coherence tomography in rheological studies: blood flow and vessels mechanical properties evaluation. J Innov Opt Health Sci. 2009; 2(4): 431–440.

23.Kokubo T, Takadama H. How useful is SBF in predicting in vivo bone bioactivity? Biomater. 2006; 27(15): 2907-2915.

24.Chlupáč J, Filova E, Bačáková L. Blood vessel replacement: 50 years of development and tissue engineering paradigms in vascular surgery. Physiol Res. 2009; 58(Suppl 2): S119-139.

25.Seifu DG, Purnama A, Mequanint K, Mantovani D. Small-diameter vascular tissue engineering. Nat Rev Cardiol. 2013; 10(7): 410.

26.Puskas JE, Chen Y. Biomedical application of commercial polymers and novel polyisobutylene-based thermoplastic elastomers for soft tissue replacement. Biomacromolecules. 2004; 5(4): 1141-1154.

27.Major R, Sanak M, Lackner JM, Bruckert F, Marczak J, Major B. Bioinspired thin film materials designed for blood contact. In Hemocomp of Biomat. for Clin. Appl. 2018 pp. 327-356. Woodhead Publishing.

28.Liu L, Wang X. Creation of a vascular system for organ manufacturing. Int J Bioprint. 2015; 1(1).

29.Hu X, Hu T, Guan G, Yu S, Wu Y, Wang L. Control of weft yarn or density improves biocompatibility of PET small diameter artificial blood vessels. J Biomed Mater Re. B. 2018; 106(3): 954-964.

30.Harper AM. Autoregulation of cerebral blood flow: influence of the arterial blood pressure on the blood flow through the cerebral cortex. J Neurol Neurosurg Psychiatry. 1966; 29(5): 398.

31.Kim BS, Park IK, Hoshiba T, Jiang HL, Choi YJ, Akaike T, Cho CS. Design of artificial extracellular matrices for tissue engineering. Prog Polym Sci. 2011; 36(2): 238-268.

32.Gunatillake PA, Adhikari R. Biodegradable synthetic polymers for tissue engineering. Eur Cell Mater. 2003; 5(1): 1-6.

33.Gao W, Wang J. Synthetic micro/nanomotors in drug delivery. Nanoscale. 2014; 6(18): 10486-10494.

34.Goodman SL, Sims PA, Albrecht RM. Three-dimensional extracellular matrix textured biomaterials. Biomater. 1996; 17(21): 2087-2095.

35.Fang J, Nakamura H, Maeda H. The EPR effect: unique features of tumor blood vessels for drug delivery, factors involved, and limitations and augmentation of the effect. Adv Drug Deliv Rev. 2011; 63(3): 136-151.

36.andeniyage LS, Gunatillake PA, Adhikari R, Bown M, Shanks R, Adhikari B. Development of high strength siloxane poly (urethane-urea) elastomers based on linked macrodiols for heart valve application. J Biomed Mater Res B. 2018; 106(5): 1712-17120.

37.Dandeniyage LS, Adhikari R, Bown M, Shanks R, Adhikari B, Easton CD, Gengenbach TR, Cookson D, Gunatillake PA. Morphology and surface properties of high strength siloxane poly (urethane-urea) s developed for heart valve application. J Biomed Mater Res B Appl Biomater. 2019; 107(1): 112-121.

38.Griffin M, Naderi N, Kalaskar DM, Malins E, Becer R, Thornton CA, Whitaker IS, Mosahebi A, Butler PE, Seifalian AM. Evaluation of sterilisation techniques for regenerative medicine scaffolds fabricated with polyurethane nonbiodegradable and bioabsorbable nanocomposite materials. Int J Biomater. 2018; 2018.

39.Lewis AL, Tolhurst LA, Stratford PW. Analysis of a phosphorylcholine-based polymer coating on a coronary stent pre-and post-implantation. Biomater. 2002; 23(7): 1697-1706.

40.Klement P, Du YJ, Berry LR, Tressel P, Chan AK. Chronic performance of polyurethane catheters covalently coated

Nanomed. J. 6(3):183-194, Summer 2019

193

with ATH complex: a rabbit jugular vein model. Biomater. 2006; 27(29): 5107-5117.

41. Campoccia D, Montanaro L, Arciola CR. A review of the biomaterials technologies for infection-resistant surfaces. Biomater. 2013; 34(34): 8533-8554.

42. Mohanty M, Kumary TV, Lal AV, Sivakumar R. Short term tissue response to carbon fibre: A preliminaryin vitro and in vivo study. Bull Mater Sci. 1998; 21(6): 439-444.

43. Ghadirinejad M, Atasoylu E, Izbirak G, Ghasemi M. A Stochastic Model for the Ethanol Pharmacokinetics. Iran J Public Health. 2016; 45(9): 1170.

44. Lee SJ, Heo DN, Park JS, Kwon SK, Lee JH, Lee JH, Kim WD, Kwon IK, Park SA. Characterization and preparation of bio-tubular scaffolds for fabricating artificial vascular grafts by combining electrospinning and a 3D printing system. Phys Chem Chem Phys. 2015; 17(5): 2996-2999.

45. Khandan A, Ozada N, Saber-Samandari S, Nejad MG. On the mechanical and biological properties of bredigite-magnetite (Ca7MgSi4O16-Fe3O4) nanocomposite scaffolds. Ceram Int. 2018; 44(3): 3141-3148.

46. Ghayour H, Abdellahi M, Nejad MG, Khandan A, Saber-Samandari S. Study of the effect of the Zn 2+ content on the anisotropy and specific absorption rate of the cobalt ferrite: the application of Co1−xZnxFe2O4 ferrite for magnetic hyperthermia. J Aust Ceram Soc. 2018; 54(2): 223-230.

47. Sahmani S, Shahali M, Nejad MG, Khandan A, Aghdam MM, Saber-Samandari S. Effect of copper oxide nanoparticles on electrical conductivity and cell viability of calcium phosphate scaffolds with improved mechanical strength for bone tissue engineering. EPJ Plus. 2019; 134(1): 7.

48. Sahmani S, Khandan A, Saber-Samandari S, Aghdam MM. Vibrations of beam-type implants made of 3D printed bredigite-magnetite bio-nanocomposite scaffolds under axial compression: Application, communication and simulation. Ceram Int. 2018; 44(10): 11282-11291.

49. Moradi-Dastjerdi R, Aghadavoudi F. Static analysis of functionally graded nanocomposite sandwich plates reinforced by defected CNT. Compos Struct. 2018;200: 839-848.

50. Aghadavoudi F, Golestanian H, Tadi Beni Y. Investigating the effects of resin crosslinking ratio on mechanical properties of epoxy-based nanocomposites using molecular dynamics. Poly Compos. 2017; 38: E433-42.

51. Aghadavoudi F, Golestanian H, Zarasvand KA. Elastic behaviour of hybrid cross-linked epoxy-based nanocomposite reinforced with GNP and CNT: experimental and multiscale modelling. Polym Bull. 2018: 1-20.

52. Monfared RM, Ayatollahi MR, Isfahani RB. Synergistic effects of hybrid MWCNT/nanosilica on the tensile and tribological properties of woven carbon fabric epoxy composites. Thero Appl Fract Mec. 2018; 96: 272-284.

53. Chan KS, Liang W, Francis WL, Nicolella DP. A multiscale modeling approach to scaffold design and property prediction. J Mech Behav Biomed. 2010; 3(8): 584-593.

194

Nanomed. J. 6(3):183-194, Summer 2019